Inorganic Chemistry

Article

pubs.acs.org/IC

Phosphorescence Color Tuning of Cyclometalated Iridium Complexes by *o*-Carborane Substitution

Taewon Kim,[†] Hyungjun Kim,[‡] Kang Mun Lee,[‡] Yoon Sup Lee,*[,‡] and Min Hyung Lee*[,†]

[†]Department of Chemistry and EHSRC, University of Ulsan, Ulsan 680-749, Republic of Korea

[‡]Department of Chemistry, KAIST, Daejeon 305-701, Republic of Korea

Supporting Information

ABSTRACT: Heteroleptic $(C^{\wedge}N)_2$Ir(acac) ($C^{\wedge}N$ = 4-*CBppy* (**1**); 5-*CBppy* (**2**), 4-*fppy* (**4**) *CB* = *ortho*-methylcarborane; *ppy* = 2-phenylpyridinato-C^2,N, 4-*fppy* = 2-(4-fluorophenyl)-pyridinato-C^2,N, acac = acetylacetonate) complexes were prepared and characterized. While **1** exhibits a phosphorescence band centered at 531 nm, which is red-shifted compared to that of unsubstituted $(ppy)_2$Ir(acac) (**3**) (λ_{em} = 516 nm), the emission spectrum of **2** shows a blue-shifted band at 503 nm. Comparison with the emission band for the 4-fluoro-substituted **4** (λ_{em} = 493 nm) indicates a substantial bathochromic shift in **1**. Electrochemical and theoretical studies suggest that while carborane substitution on the 4-position of the phenyl ring lowers the ^{3}MLCT energy by a large contribution to lowest unoccupied molecular orbital (LUMO) delocalization, which in turn assigns the lowest triplet state of **1** as $[d_\pi(Ir)\rightarrow\pi^*(C^{\wedge}N)]$ ^{3}MLCT in character, the substitution on the 5-position raises the ^{3}MLCT energy by the effective stabilization of the highest occupied molecular orbital (HOMO) level because of the strong inductive effect of carborane. An electroluminescent device incorporating **1** as an emitter displayed overall good performance in terms of external quantum efficiency (6.6%) and power efficiency (10.7 lm/W) with green phosphorescence.

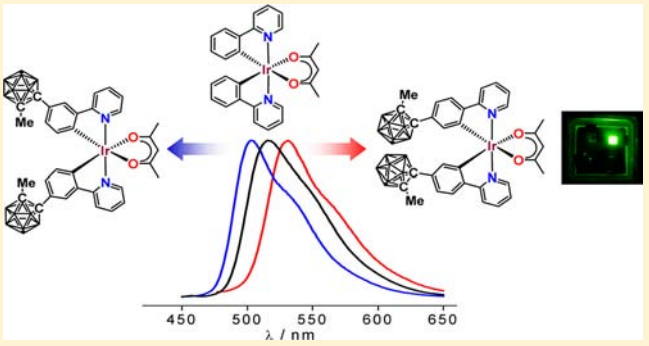

INTRODUCTION

Phosphorescent heavy metal complexes have attracted a great deal of interest as emitting materials in organic light-emitting diodes (OLEDs) because of their excellent properties such as good color purity, high quantum efficiency, relatively short phosphorescence lifetime, and high photo- and thermal stability.[1,2] In particular, modification of the cyclometalating ligand ($C^{\wedge}N$ ligand) has enabled control of emission color over the entire visible region that can be beneficial for realizing full-color and white-light displays.[3] The tuning of phosphorescence color has usually been achieved by the variation of the substituent on the $C^{\wedge}N$ ligand, for example, *ppy* (2-phenylpyridinato-C^2,N), since the emissive lowest-energy excited states such as ^{3}MLCT and $^3\pi-\pi^*$ (^{3}LC) are largely involved with the electronic structure of the ligand.[4−8]

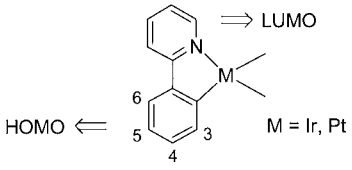

Experimental and theoretical studies reported to date have established the basic principles for the emission color control as follows:[6−10] (i) the highest occupied molecular orbital (HOMO) level of the complex is dominated by the π orbital of the phenyl ring of the *ppy* ligand together with the metal t_{2g} manifold (d_π orbitals) and (ii) the π^* orbital of the pyridyl ring of the *ppy* ligand governs the lowest unoccupied molecular orbital (LUMO) level. Consequently, the introduction of an electron-withdrawing group such as a fluorine atom into the phenyl ring of the ligand usually gives rise to an increase in the HOMO−LUMO band gap by lowering the HOMO level, while introduction into the pyridyl ring narrows the band gap by lowering the LUMO level. As a result, the energy level of the triplet state formed from the HOMO−LUMO transition can be fine-tuned in accordance with the change in the band gap. Moreover, the orbital analyses further suggest that the position of the substituent on each ring of ligand is also important for tuning the emission wavelength.[9] For example, the electron-withdrawing effect of a fluorine atom attached on the 4- and/or 6-carbon positions of the phenyl ring gives a large blue shift by the greater HOMO stabilization than LUMO, but substitution at the 5-position offsets the electron-withdrawing effect of the fluorine atom by weak π-donation from fluorine into the electron density of the HOMO at this position, thereby reducing the band gap.

Although these approaches to phosphorescence color tuning by use of the electron-donating or -withdrawing substituents

Received: July 18, 2012
Published: December 20, 2012

   dx.doi.org/10.1021/ic3015699 | *Inorg. Chem.* 2013, 52, 160−168

have been well established, it is still highly desirable to develop phosphors whose emitting properties can be easily tuned by modification of the electronic structure of the ligand. In an effort to design a novel family of color-tunable phosphors, we have been interested in 1,2-*closo*-$C_2B_{10}H_{12}$, so-called *o*-carborane as a substituent since it possesses unique properties such as a highly polarizable σ-aromatic character, electron-deficient nature, and good thermal and chemical stability.[11] Owing to these interesting properties, *o*-carborane has recently received attention in the field of fluorescent materials.[12] In particular, we have recently demonstrated that when incorporated into an organic π-system such as triarylborane, *o*-carborane significantly stabilizes a LUMO level by direct contribution to LUMO delocalization, as well as by a strong inductive electron-withdrawing effect.[13,14] The bulkiness of *o*-carborane may also hinder the intermolecular interactions between phosphorescent emitter molecules and thereby suppress triplet−triplet annihilation and concentration quenching in solid state. These properties of carborane led us to consider whether the substitution of an *o*-carborane into the *C^N* ligand could exert an effect on the emission color tuning of an Ir(III) complex.

In this report, we introduced an *o*-carborane into the 4- or 5-position of the phenyl ring of the *ppy* ligand and investigated the photophysical properties of Ir(III) complexes (**1** and **2** in Chart 1). We find that a simple change in the position of

Chart 1

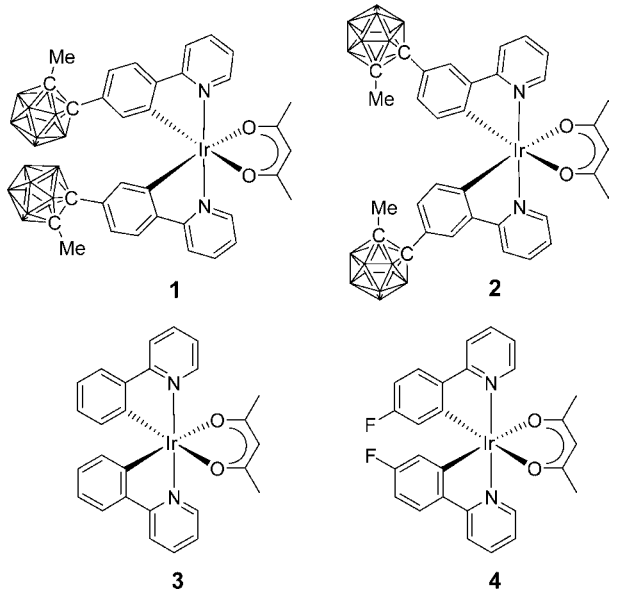

carborane substitution on the phenyl ring leads to facile tuning of emission wavelength from red to blue shift with respect to that of the unsubstituted $(ppy)_2$Ir(acac) complex (**3**). Synthesis, characterization, and photophysical and electroluminescent properties of carborane-substituted heteroleptic Ir(III) complexes **1** and **2** are described with theoretical calculations.

EXPERIMENTAL SECTION

Chemical and Instrumentation. All operations were performed under an inert nitrogen atmosphere using standard Schlenk and glovebox techniques. Anhydrous grade solvents (Aldrich) were dried by passing them through an activated alumina column and stored over activated molecular sieves (5 Å). Spectrophotometric grade dichloromethane and toluene (Aldrich) were used as received. Commercial reagents were used without any further purification after purchasing from Aldrich (2-bromopyridine, *n*-BuLi (2.5 M solution in *n*-hexanes), 1-bromo-4-iodobenzene, 1-bromo-3-iodobenzene, ethynyl(trimethyl)-silane, KOH, diethyl sulfide, lithium diisopropylamide (2.0 M in THF), MeI, 2,4-pentanedione (acacH), Na_2CO_3, quinine sulfate), Strem (iridium(III) chloride hydrate, $Pd(PPh_3)_4$), TCI (Me_3SnCl), Katchem (Decaborane), and Lumtec (*fac*-Ir(ppy)$_3$, >99%, sublimed grade). 3-Bromophenylacetylene,[15] 2-(trimethylstannyl)pyridine,[16] 1-(4-bromophenyl)-2-methyl-1,2-*closo*-carborane (**1a**),[14] $(ppy)_2$Ir-(acac),[7] and $[(4\text{-}fppy)_2Ir(\mu\text{-}Cl)]_2$[17] were synthesized according to the reported procedures. Deuterated solvents from Cambridge Isotope Laboratories were used. NMR spectra were recorded on a Bruker 300 a.m. spectrometer (300.13 MHz for ^{1}H, 75.48 MHz for ^{13}C, 96.29 MHz for ^{11}B) at ambient temperature. Chemical shifts are given in parts per million (ppm), and are referenced against external Me_4Si (^{1}H, ^{13}C) and $BF_3{\cdot}OEt_2$ (^{11}B). Elemental analyses were performed on an EA1110 (FISONS Instruments) by the Environmental Analysis Laboratory at KAIST. HR EI−MS measurement (JEOL JMS700) was carried out at Korea Basic Science Institute. UV−vis absorption and PL spectra were recorded on a Varian Cary 100 and a HORIBA FluoroMax-4P spectrophotometer, respectively. Lifetime measurements were carried out with an Edinburgh FLS 920 spectrophotometer equipped with Xenon microsecond flashlamp. Cyclic voltammetry experiment was performed using an AUTOLAB/PGSTAT101 system.

Synthesis of 1-(3-BrPh)-2-Me-1,2-*closo*-$C_2B_{10}H_{10}$ (2a). This compound was prepared in a manner analogous to the synthesis of **1a**.[14] To a toluene solution (50 mL) of decaborane ($B_{10}H_{14}$, 2.47 g, 13.6 mmol) and 3-bromophenylacetylene (2.00 g, 16.3 mmol) was added an excess amount of Et_2S (5 equiv) at room temperature. The reaction mixture was stirred at reflux for 3 d. The solvent was removed, and the resulting solid residue was purified by column chromatography on alumina, affording 1-(3-BrPh)-1,2-*closo*-$C_2B_{10}H_{11}$ as a white solid. Yield: 2.41 g, 59%. ^{1}H NMR ($CDCl_3$): δ 7.52 (t, J = 2.0 Hz, 1H, Ph−C*H*), 7.51 (dt, J = 8.1, 2.0 Hz, 1H, Ph−C*H*), 7.40 (dt, J = 8.1, 2.0 Hz, 1H, Ph−C*H*), 7.18 (t, J = 8.1 Hz, 1H, Ph−C*H*), 3.93 (s, 1H, C*H*), 1.3−3.5 (br, 10H, B−*H*). ^{13}C NMR ($CDCl_3$): δ 135.6, 133.3, 130.8, 130.5, 126.5, 123.1, 75.2, 60.2 ($C_2B_{10}H_{10}$). ^{11}B NMR ($CDCl_3$): −2.0, −4.1, −8.9, −11.0, −12.7. HR EI-MS: m/z calcd for $C_8H_{15}B_{10}Br$, 300.1288; found, 300.1291.

Next, the solution of 1-(3-BrPh)-1,2-*closo*-$C_2B_{10}H_{11}$ (2.23 g, 7.64 mmol) in tetrahydrofuran (THF) was treated with lithium diisopropylamide (4.20 mL, 8.40 mmol) at 0 °C. After stirring for an additional 1 h, an excess amount of MeI (3 equiv, 25.2 mmol) was added into the mixture at 0 °C. The reaction mixture was allowed slowly to reach room temperature and was stirred for 2 h. After quenching the reaction with water (30 mL), the aqueous layer was extracted with ether (3 × 30 mL). The organic layers were separated, dried over $MgSO_4$, and concentrated under reduced pressure. Purification by column chromatography on alumina afforded 1-(3-BrPh)-2-Me-1,2-*closo*-$C_2B_{10}H_{10}$ (**2a**) as a white solid. Yield: 1.79 g, 75%. ^{1}H NMR ($CDCl_3$): δ 7.77 (t, J = 2.0 Hz, 1H, Ph−C*H*), 7.59 (dt, J = 8.1, 2.0 Hz, 2H, Ph−C*H*), 7.26 (t, 1H, J = 8.1 Hz Ph−C*H*), 1.67 (s, 3H, B−CH_3), 1.3−3.5 (br, 10H, B−*H*). ^{13}C NMR ($CDCl_3$): δ 134.2, 134.0, 133.2, 130.5, 129.9, 123.2 (Ph-*C*), 80.8, 77.5 ($C_2B_{10}H_{10}$), 23.4 (B-CH_3). ^{11}B NMR ($CDCl_3$): −2.8, −4.5, −10.1. HR EI-MS: m/z calcd for $C_9H_{17}B_{10}Br$, 314.1444; found, 314.1448.

Synthesis of 2-{*p*-(2-Me-1,2-carboran-1-yl)phenyl}pyridine (4-*CBppyH*, 1b). **1a** (1.75 g, 5.57 mmol), 2-(trimethylstannyl)-pyridine (1.48 g, 6.13 mmol), and $Pd(PPh_3)_4$ (0.13 g, 2.0 mol %) were dissolved in toluene (70 mL), and the solution was heated to reflux overnight. After cooling to room temperature, the reaction mixture was quenched by addition of saturated aqueous NH_4Cl. The organic phase was separated and the aqueous layer was further extracted with Et_2O (30 mL). The combined organic layers were dried over $MgSO_4$, and concentrated under reduced pressure. The residue was purified by flash column chromatography using CH_2Cl_2/toluene (1/1, v/v) as an eluent. Drying in vacuo afforded **1b** as a white solid (1.03 g, 54%). ^{1}H NMR ($CDCl_3$): δ 8.70 (dq, 1H, J = 4.8, 0.9 Hz), 7.99 (dt, 2H, J = 8.7,

dx.doi.org/10.1021/ic3015699 | Inorg. Chem. 2013, 52, 160−168

Table 1. Photophysical and Electrochemical Data for 1−4

compound (C^N)	λ_{abs}/nm ($\varepsilon \times 10^{-3}$/M^{-1} cm^{-1})[a]	λ_{em}/nm[a] 298 K	λ_{em}/nm[a] 77 K	τ/μs[a]	Φ_{em}[a,b]	E_{ox}/V[c] (ΔE_p/mV)	E_{red}/V[c] (ΔE_p/mV)
1 (4-*CBppy*)	261 (38.3), 279 (38.1), 353 (5.4), 390 (3.4), 415 (2.7), 474 (2.0), 509 (0.5)	531	524	3.0	0.02	0.51 (90)[e]	−2.12 (270)[f]
2 (5-*CBppy*)	256 (48.4), 274 (43.1), 299 (33.4), 342 (10.1), 378 (4.8), 401 (3.9), 451 (2.4), 481 (1.0)	503	493	0.6	0.15	0.55 (140)[e]	−2.19 (360)[f]
3 (*ppy*)	260 (47.1), 339 (8.4), 405 (3.5), 460 (2.4), 491 (0.6)	516	502	1.6[d]	0.34[d]	0.41[g]	−2.60[g]
4 (4-*fppy*)	259 (40.9), 287 (29.5), 331 (11.3), 393 (5.0), 444 (2.5), 474 (0.8)	493	483	1.5	0.40	0.46 (100)[e]	*h*

[a]Measured in degassed CH_2Cl_2 (~ 10^{-5} M). [b]Quinine sulfate (0.5 M H_2SO_4) as a standard (Φ = 0.55).[19] [c]Measured in DMF (1 mM, scan rate =100 mV/s) with reference to a Fc/Fc^+ redox couple. [d]Data from ref 7. [e]Reversible oxidation. [f]Quasi-reversible reduction. [g]Data from ref 31. [h]Not observed.

2.1 Hz), 7.70−7.80 (m, 4H), 7.27 (ddd, 1H, *J* = 6.9, 4.8, 1.5 Hz), 1.70 (s, 3H, B−CH_3), 1.50−3.70 (br, 10H, B−*H*). ^{13}C NMR ($CDCl_3$): δ 155.7, 149.9, 141.5, 137.1, 131.5, 131.3, 127.3, 123.0, 120.8 (ppy-*C*), 81.8, 77.4 ($C_2B_{10}H_{10}$), 23.2 (B-CH_3). ^{11}B NMR ($CDCl_3$): −3.0, −4.4, −10.0. HR EI-MS: *m*/*z* calcd for $C_{14}H_{21}B_{10}N$, 313.2605; found, 313.2606.

Synthesis of 2-{*m*-(2-Me-1,2-carboran-1-yl)phenyl}pyridine (5-*CBppyH*, 2b). This compound was prepared in a manner analogous to the synthesis of **1b** using **2a** (1.79 g, 5.72 mmol), 2-(trimethylstannyl)pyridine (1.66 g, 6.87 mmol), and $Pd(PPh_3)_4$ (0.13 g, 2.0 mol %). Yield: 1.24 g, 70%. ^{1}H NMR ($CDCl_3$): δ 8.71 (dq, 1H, *J* = 4.8, 1.8 Hz), 8.30 (t, 1H, *J* = 1.8 Hz), 8.03 (dt, 1H, *J* = 7.8, 1.2 Hz), 7.81 (td, 1H, *J* = 7.8, 1.8 Hz), 7.70 (tt, 2H, *J* = 7.8, 1.2 Hz), 7.48 (t, 1H, *J* = 7.8 Hz), 7.27 (dd, 1H, *J* = 4.8, 1.2 Hz), 1.72 (s, 3H, B−CH_3), 1.50−3.70 (br, 10H, B−*H*). ^{13}C NMR ($CDCl_3$): δ 156.1, 150.2, 140.5, 137.2, 131.7, 131.5, 130.0, 129.5, 129.1, 123.0, 120.9 (ppy-*C*), 82.3 77.5 ($C_2B_{10}H_{10}$), 23.5 (B-CH_3). ^{11}B NMR ($CDCl_3$): δ −3.0, −4.5, −10.0 . HR EI-MS: *m*/*z* calcd for $C_{14}H_{21}B_{10}N$, 313.2605; found, 313.2605.

Synthesis of [(4-*CBppy*)$_2$Ir(μ-Cl)]$_2$ (1c). 1b (1.03 g, 3.29 mmol) and $IrCl_3 \cdot 3H_2O$ (0.51 g, 1.43 mmol) were dissolved in the mixed solvent of 2-ethoxyethanol (40 mL) and distilled water (20 mL). The reaction mixture was heated to 110 °C and stirred for 1 d. After cooling to room temperature, 30 mL of distilled water was added to precipitate out the solid materials. The precipitate was filtered and washed with small portions of ethanol (2 × 10 mL). The crude solid was extracted with CH_2Cl_2, and the solution was dried over $MgSO_4$. Filtration followed by drying in vacuo gave a light yellow solid of **1c**. Yield: 1.07 g, 88%. ^{1}H NMR ($CDCl_3$): δ 9.31 (d, 4H, *J* = 5.7 Hz), 7.92 (m, 8H), 7.44 (d, 4H, *J* = 8.4 Hz), 7.01 (m, 8H), 6.01 (d, 4H, *J* = 1.8 Hz), 1.33 (s, 12H, B−CH_3), 1.20−3.50 (br, 40H, B−*H*). ^{13}C NMR ($CDCl_3$): δ 167.1, 151.7, 145.9, 144.1, 137.4, 132.7, 130.6, 124.4, 123.4, 123.2, 120.0, 82.0, 71.5 ($C_2B_{10}H_{10}$), 22.9 (B-CH_3). ^{11}B NMR ($CDCl_3$): δ −4.3, −9.5. Anal. Calcd for $C_{56}H_{80}B_{40}Cl_2Ir_2N_4$: C, 39.63; H, 4.75; N, 3.30. Found: C, 39.63; H, 4.81; N, 3.27.

Synthesis of [(5-*CBppy*)$_2$Ir(μ-Cl)]$_2$ (2c). This compound was prepared in a manner analogous to the synthesis of **1c** using **2b** (1.24 g, 3.99 mmol) and $IrCl_3 \cdot 3H_2O$ (0.61 g, 1.73 mmol). Yield: 1.46 g, 93%. ^{1}H NMR ($CDCl_3$): δ 9.08 (d, 4H, *J* = 5.7 Hz), 7.88 (m, 8H), 7.69 (s, 4H), 6.88 (t, 4H, *J* = 6.6 Hz), 6.79 (d, 4H, *J* = 8.1 Hz), 5.90 (d, 4H, *J* = 8.1 Hz), 1.53 (s, 12H, B−CH_3), 1.20−3.50 (br, 40H, B−*H*). ^{13}C NMR (acetone-d_6): δ 167.9, 153.1, 151.2, 147.1, 139.8, 132.5, 132.4, 127.3, 125.9, 125.4, 121.5, 85.5, 79.7 ($C_2B_{10}H_{10}$), 22.9 (B-CH_3). ^{11}B NMR ($CDCl_3$): δ −4.4, −10.1. Anal. Calcd for $C_{56}H_{80}B_{40}Cl_2Ir_2N_4$: C, 39.63; H, 4.75; N, 3.30. Found: C, 39.38; H, 4.37; N, 3.09.

Synthesis of (4-*CBppy*)$_2$Ir(acac) (1). Into the flask containing the dimeric iridium(III) complex **1c** (1.07 g, 0.63 mmol), 2,4-pentanedione (0.19 g, 1.90 mmol), and Na_2CO_3 (0.67 g, 6.32 mmol) was added acetonitrile (50 mL). The reaction mixture was heated to 80 °C and stirred for 2 d. After cooling to room temperature, the orange precipitate formed was collected by filtration and washed with acetonitrile (10 mL). The crude solid was extracted with CH_2Cl_2 to remove remaining salts. The solution was dried over $MgSO_4$ and filtered. Evaporation of solvent followed by drying in vacuo afforded orange solid of **1**. Yield: 0.95 g, 83%. Single crystals suitable for X-ray diffraction study were obtained from slow evaporation of an acetone/MeOH solution of **1**. ^{1}H NMR ($CDCl_3$): δ 8.50 (d, 2H, *J* = 6.0 Hz), 7.87 (m, 4H), 7.42 (d, 2H, *J* = 8.4 Hz), 7.30 (td, 2H, *J* = 6.0, 2.7 Hz), 6.94 (dd, 2H, *J* = 8.4, 2.1 Hz), 6.22 (d, 2H, *J* = 2.1 Hz), 5.31 (s, 1H, acac-C*H*), 1.83 (s, 6H, acac-CH_3), 1.14 (s, 6H, B−CH_3), 1.10−3.00 (br, 20H, B−*H*). ^{13}C NMR (CD_2Cl_2): δ 185.7 (acac-*C*O), 167.2, 149.2, 147.9, 147.8, 138.5, 135.0, 130.4, 124.5, 123.8, 123.6, 120.0, 101.2 (acac-CH), 83.2, 77.9 ($C_2B_{10}H_{10}$), 28.8 (acac-CH_3), 22.9 (B-CH_3). ^{11}B NMR ($CDCl_3$): δ −4.8 (br, 4B), −10.4 (br, 6B). Anal. Calcd for $C_{33}H_{47}B_{20}IrN_2O_2$: C, 43.45; H, 5.19; N, 3.07. Found: C, 43.38; H, 5.19; N, 3.08.

Synthesis of (5-*CBppy*)$_2$Ir(acac) (2). This compound was prepared in a manner analogous to the synthesis of **1** using **2c** (1.37 g, 0.81 mmol), 2,4-pentanedione (0.24 g, 2.43 mmol), and sodium carbonate (0.86 g, 8.09 mmol). Yield: 1.40 g, 95%. ^{1}H NMR ($CDCl_3$): δ 8.48 (d, 2H, *J* = 5.4 Hz), 7.92 (d, 2H, *J* = 8.1 Hz), 7.83 (dt, 2H, *J* = 8.4, 1.5 Hz), 7.71 (d, 2H, *J* = 2.1 Hz), 7.23 (m, 2H), 6.87 (dd, 2H, *J* = 8.1, 2.1 Hz), 6.22 (d, 2H, *J* = 8.1 Hz), 5.23 (s, 1H, acac-C*H*), 1.79 (s, 6H, acac-CH_3), 1.57 (s, 6H, B−CH_3), 1.10−3.10 (br, 20H, B−*H*). ^{13}C NMR (CD_2Cl_2): δ 185.4 (acac-*C*O), 167.0, 152.5, 148.7, 146.5, 138.1, 134.0, 131.2, 126.2, 123.7, 123.2, 119.4, 100.9 (acac-CH), 84.1, 78.1 ($C_2B_{10}H_{10}$), 28.5 (acac-CH_3), 23.3 (B-CH_3). ^{11}B NMR ($CDCl_3$): δ −4.5 (br, 4B), −10.1 (br, 6B). Anal. Calcd for $C_{33}H_{47}B_{20}IrN_2O_2$: C, 43.45; H, 5.19; N, 3.07. Found: C, 43.56; H, 5.21; N, 3.06.

Synthesis of (4-*fppy*)$_2$Ir(acac) (4). This compound was prepared in a manner analogous to the synthesis of **1** using [(4-*fppy*)$_2$Ir(μ-Cl)]$_2$ (0.176 g, 0.154 mmol), 2,4-pentanedione (0.039 g, 0.385 mmol), and sodium carbonate (0.163 g, 1.54 mmol). Yield: 0.122 g, 62%. ^{1}H NMR (CD_2Cl_2): δ 8.43 (dt, 2H, *J* = 4.2 Hz), 7.80 (m, 4H), 7.59 (dd, 2H, *J* = 8.7, 5.7 Hz), 7.21 (dt, 2H, *J* = 6.0, 2.1 Hz), 6.58 (dt, 2H, *J* = 8.7, 2.7 Hz), 5.87 (dd, 2H, *J* = 9.9, 2.7 Hz), 5.30 (s, 1H), 1.80 (s, 6H). ^{13}C NMR (CD_2Cl_2): 185.5 (acac-*C*O), 148.7, 138.1, 126.1, 126.0, 122.4, 119.6, 119.3, 119.2, 108.7, 108.4, 101.0 (acac-CH), 28.8 (acac-CH_3). Anal. Calcd for $C_{27}H_{21}F_2IrN_2O_2$: C, 51.01; H, 3.33; N, 4.41. Found: C, 50.99; H, 3.62; N, 4.21.

X-ray Crystallography. A specimen of suitable size and quality was coated with Paratone oil and mounted onto a glass capillary. The crystallographic measurement was performed using a Bruker Apex II-CCD area detector diffractometer, with graphite-monochromated Mo*K*α radiation (λ = 0.71073 Å). The structure was solved by direct methods, and all nonhydrogen atoms were subjected to anisotropic refinement by full-matrix least-squares on F^2 by using the SHELXTL/PC package.[18] Hydrogen atoms were placed at their geometrically calculated positions and were refined riding on the corresponding carbon atoms with isotropic thermal parameters. The detailed crystallographic data are given in Supporting Information, Table S1.

UV−vis Absorption and PL Measurements. UV−visible absorption and photoluminescence (PL) measurements were performed in degassed CH_2Cl_2 with a 1-cm quartz cuvette. PL quantum efficiencies were measured with reference to that of quinine sulfate in 0.5 M H_2SO_4 (Φ = 0.55)[19] and were calculated according to the following equation, which includes refractive index correction:

dx.doi.org/10.1021/ic3015699 | *Inorg. Chem.* 2013, 52, 160−168

Scheme 1[a].

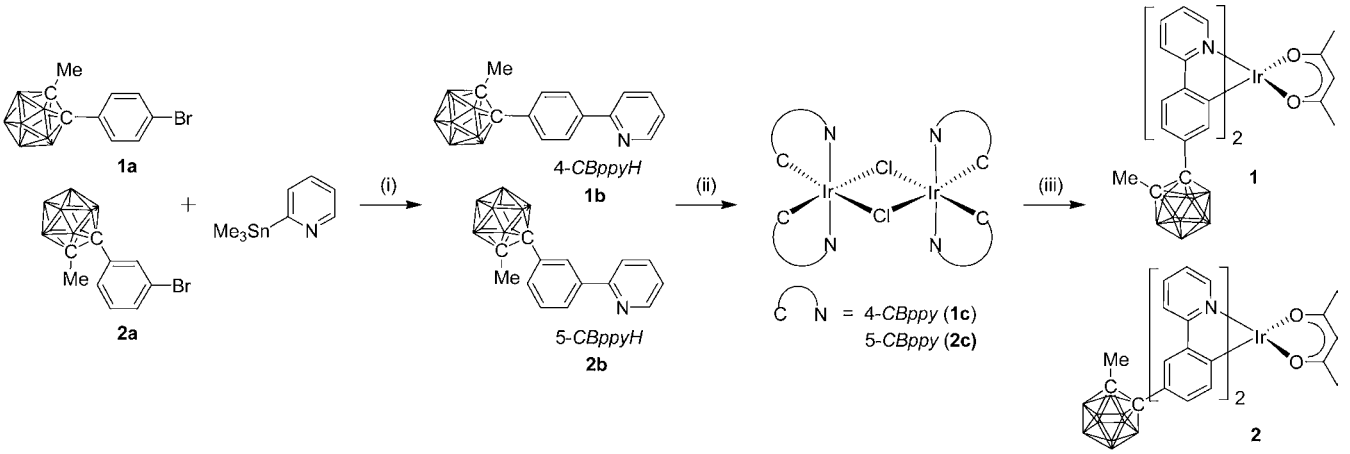

[a]Conditions: (i) $Pd(PPh_3)_4$, toluene, 110 °C, 54% (**1b**) and 70% (**2b**). (ii) $IrCl_3 \cdot 3H_2O$, 2-ethoxyethanol/H_2O, 110 °C, 88% (**1c**) and 93% (**2c**). (iii) 2,4-Pentanedione, Na_2CO_3, acetonitrile, 80 °C, 83% (**1**) and 95% (**2**).

$$\Phi_s = \Phi_r\left(\frac{\eta_s^2 A_r I_s}{\eta_r^2 A_s I_r}\right)$$

where Φ is the quantum efficiency; η is the refractive index of the solvent; A is absorbance at the excitation wavelength; I is the integrated area under the emission spectrum; and the subscripts s and r refer to the sample and reference, respectively. The η values of 1.424 for CH_2Cl_2 and 1.346 for 0.5 M H_2SO_4[20] were used in the calculation. The detailed conditions for absorption and PL measurements are given in the figure captions and Table 1.

Cyclic Voltammetry. Cyclic voltammetry measurements were carried out in dimethylformamide (DMF, 1 mM) with a three-electrode cell configuration consisting of platinum working and counter electrodes and a $Ag/AgNO_3$ (0.01 M in CH_3CN) reference electrode at room temperature. Tetra-*n*-butylammonium hexafluorophosphate (0.1 M) was used as the supporting electrolyte. The redox potentials were recorded at a scan rate of 100 mV/s and are reported with reference to the ferrocene/ferrocenium (Fc/Fc^+) redox couple.

Fabrication of Electroluminescent Devices. The configuration of EL devices is as follows: ITO/NPB (40 nm)/CBP:emitter (8 wt %) (30 nm)/BCP (10 nm)/Alq_3 (40 nm)/LiF (1 nm)/Al (100 nm), where emitter is **1** or *fac*-$Ir(ppy)_3$; NPB is *N*,*N*′-bis(naphthalene-1-yl)-*N*,*N*′-bis(phenyl)-benzidine (EM Index, a local company in Korea, >99%, sublimed grade); CBP is 4,4′-bis(9-carbazolyl)-biphenyl (Nichem, >99%, sublimed grade); BCP is bathocuproine (Lumtec, >99.8%, sublimed grade); Alq_3 is tris(8-hydroxyquinolinolato) aluminum (EM Index, >99%, sublimed grade). Onto a glass substrate precoated with ITO, a hole-transporting NPB layer was deposited using the vacuum evaporation method (~10^{-7} Torr). A layer of CBP host was subsequently codeposited with an emitter material under high vacuum. The film thickness of the EML was determined with a TENCOR alpha-step 500 profiler. Hole-blocking BCP, electron transporting Alq_3 layers, and a cathode layer of LiF and Al were successively deposited on top of the EML (deposition rates: BCP, Alq_3 = 1 Å/s, LiF = 0.1 Å/s, Al electrode = 3 Å/s). EL spectra were obtained with a PR-650 spectrometer. Current–voltage (J–V) and luminance–voltage (L–V) characteristics were recorded on a current–voltage source (Keithley 237) and a luminescence detector (PR-650). All EL measurements were carried out in an N_2-filled glovebox at room temperature.

Theoretical Calculations. The geometries of the ground (S_0) and lowest-lying triplet excited (T_1) states of **1** were optimized using the density functional theory (DFT) method. The electronic transition energies including electron correlation effects were computed by the time dependent density functional theory (TD-DFT)[21] method using the B3LYP[22] functional (TD-B3LYP). The 6-31G(d) basis set[23] was used for all atoms except for the iridium atom which was treated with LANL2DZ effective core potentials (ECPs) and corresponding basis sets.[24] All calculations described here were carried out using the GAUSSIAN 09 program.[25]

RESULTS AND DISCUSSION

Synthesis and Characterization. The *ortho*-methylcarborane (*CB*) substituted 2-phenylpyridine ligands, 4-*CBppyH* (**1b**)

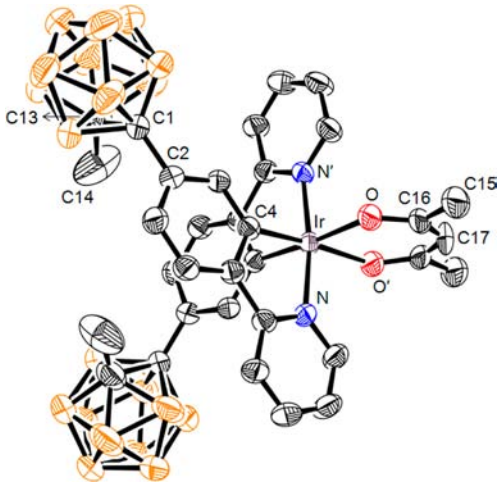

Figure 1. Crystal structure of **1** (40% thermal ellipsoids). H-atoms are omitted for clarity. Selected bond lengths (Å) and angles (deg): Ir–N 2.047(4), Ir–C(4) 1.987(5), Ir–O 2.161(3), C(1)–C(2) 1.514(7), C(1)–C(13) 1.697(8), N–Ir–N′ 171.9(2), O–Ir–O′ 87.0(2), N–Ir–C(4) 80.5(2).

and 5-*CBppyH* (**2b**) were prepared in moderate yield from Stille coupling reactions between 2-(trimethylstannyl)pyridine and *para*- or *meta*-carborane substituted bromobenzene (**1a** and **2a**) (Scheme 1). The starting **1a** and **2a** can easily be accessed by the reaction of arylalkyne with $B_{10}H_{14}$ in the presence of weak base such as Et_2S, MeCN, and *N*,*N*-dimethylaniline,[26] followed by alkylation of the resulting 1-Ar-2-H-1,2-*closo*-carborane using alkyl halides (Supporting Information, Scheme S1).[14,27] Because of susceptibility of carborane toward nucleophilic anions such as hydroxide at elevated temperature, the normal Suzuki–Miyaura coupling reaction under aqueous basic conditions could not be applied

dx.doi.org/10.1021/ic3015699 | Inorg. Chem. 2013, 52, 160–168

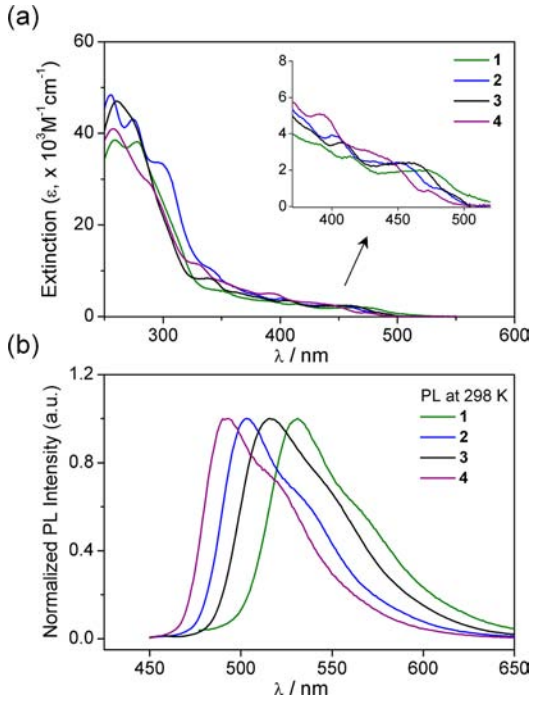

Figure 2. (a) UV–vis absorption and (b) PL spectra of **1**–**4** in degassed CH_2Cl_2 at room temperature. The inset shows the enlarged absorption spectra at the lower energy region.

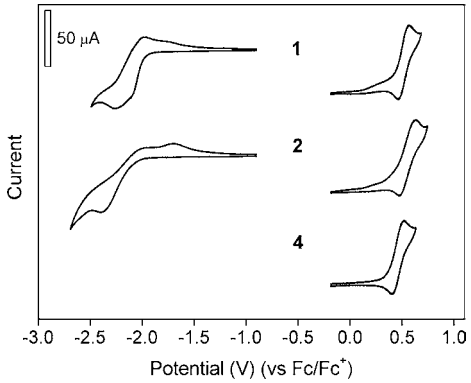

Figure 3. Cyclic voltammograms of **1**, **2**, and **4** (1 mM in DMF, scan rate = 100 mV/s).

to the synthesis of the ligands. The cyclometalation reactions of iridium(III) chloride with **1b** and **2b** afforded the chloro-bridged dimeric iridium(III) complexes, $[(C^\wedge N)_2Ir(\mu\text{-}Cl)_2Ir(C^\wedge N)_2]$ ($C^\wedge N$ = 4-*CBppy* (**1c**); 5-*CBppy* (**2c**)) in high yield. Since the cyclometalation reaction is highly sensitive to steric effects,[28] one can expect the regioselective cyclometalation of the ligand **2b** with Ir(III) at the 2-position of the phenyl ring. Spectroscopic data also reveal the formation of a single regioisomer **2c**. Treatment of **1c** and **2c** with acetylacetone (acacH) under mild basic conditions[29] cleanly led to the heteroleptic Ir(III) complexes, $(4\text{-}CBppy)_2Ir(acac)$ (**1**) and $(5\text{-}CBppy)_2Ir(acac)$ (**2**) in high yield. For comparison purpose, the 4-fluorine substituted Ir(III) complex, $(4\text{-}fppy)_2Ir(acac)$ (**4**) was analogously prepared.

Complexes **1** and **2** have been characterized by NMR spectroscopy, elemental analysis, and X-ray diffraction method. ^1H and ^{13}C NMR spectra show the expected resonances corresponding to the $(C^\wedge N)_2Ir(acac)$. Two broad ^{11}B NMR

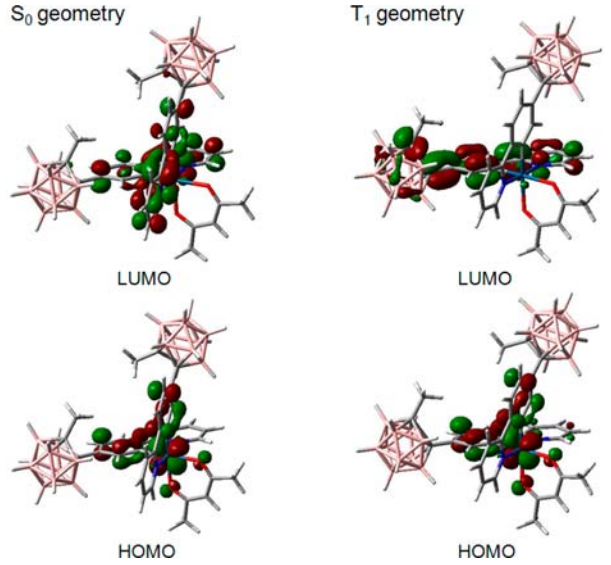

Figure 4. HOMO and LUMO of **1** at the ground state (S_0) (left) and lowest triplet excited state (T_1) (right) optimized geometries (isovalue = 0.04).

Table 2. Energy Levels and Orbital Analyses of the Excited States for 1 from TD-DFT Calculations[a]

states	λ_{calc}	f	assignment
T_1	525.5[b]	0	HOMO→LUMO (90.5%)
S_1	451.5	0.0385	HOMO→LUMO (96.0%)
S_2	442.4	0.0014	HOMO→LUMO+1 (96.0%)
S_3	399.7	0.0225	HOMO-1→LUMO+1 (95.5%)
S_4	399.4	0.0024	HOMO-1→LUMO (95.0%)

[a]Singlet energies for the vertical transition calculated at the optimized S_0 geometries. [b]Triplet energy for the adiabatic transition corresponding to the 0–0 phosphorescence.

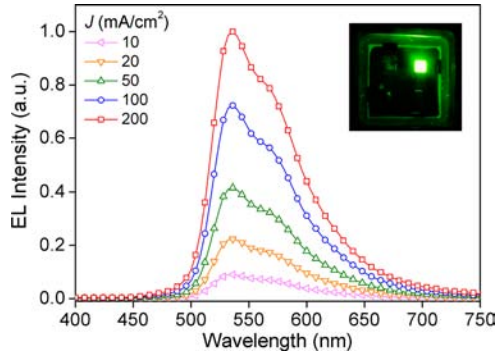

Figure 5. EL spectra of device (**D1**) fabricated with CBP host doped with **1** (8 wt %) as an emitter with respect to the current density. Inset shows a photograph of the working device (cell area: 2 × 2 mm^2).

signals centered at δ −5 and −10 ppm in a 4:6 ratio confirm the presence of *closo*-carborane. An X-ray diffraction study revealed the molecular structure of **1**. As shown in Figure 1, complex **1** which crystallizes in space group $C2/c$ adopts a Λ-configuration. The molecule possesses a C_2-axis connecting Ir and C17 atoms (Supporting Information, Figure S1). The chelating 4-*CBppy* ligands are in a trans disposition of the pyridine rings, similar to those observed in usual heteroleptic Ir(III) complexes[1,7,8,30] Geometrical parameters such as bond

dx.doi.org/10.1021/ic3015699 | Inorg. Chem. 2013, 52, 160–168

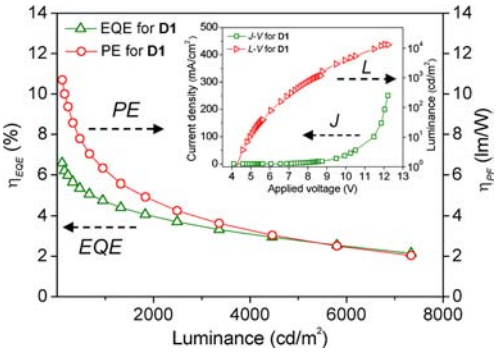

Figure 6. External quantum efficiency–luminance (η_{EQE}–L) and power efficiency–luminance (η_{PE}–L) curves of device **D1**. Inset shows the current density–applied voltage–luminance (J–V–L) characteristics of **D1**.

lengths and angles around the Ir atom are also in a similar range reported for other $(C^{\wedge}N)_2$Ir(acac) complexes.[5,7,31]

Photophysical Properties. To examine the photophysical properties, UV–vis absorption and PL experiments were carried out with **1** and **2** in degassed CH_2Cl_2 (Figure 2 and Table 1). For comparison, the spectra of **3** and **4** were also obtained. Compound **1** features an intense absorption band in the region of 250–350 nm, which can be assigned to the spin-allowed $^1\pi$–π^* transition of the 4-*CBppy* ligand (^{1}LC). The structured band shape and band energy, as well as the high extinction coefficient, are consistent with those observed for the free ligand, 4-*CBppyH* (**1b**) (Supporting Information, Figure S2). A similar $^1\pi$–π^* transition band with a slight blue shift is also observed for **2**. While the lower energy band of **1** at 415 nm results from spin-allowed metal-to-ligand charge transfer (^{1}MLCT), the band at 474 nm, which tails to over 500 nm, can be majorly assigned to a mixture of spin-forbidden MLCT (^{3}MLCT) and the $^3\pi$–π^* transition of the 4-*CBppy* ligand (^{3}LC).[8,32] It is notable that the MLCT bands for **1** are significantly red-shifted compared to those of **4** bearing a 4-fluorine atom (393 and 444 nm) and are even lower in energy than those for **3** (405 and 460 nm). In contrast, the lowest-energy bands for **2** are observed at the apparently blue-shifted region (401 and 451 nm) compared to those for **1** and **3**. These findings indicate that carborane substitution on the 4-position of the phenyl ring lowers the excited state energy, while the same substitution on the 5-position raises it (vide infra).

An identical trend in the excited state energy is also found in the PL spectra of complexes. While **1** exhibits an emission band centered at 531 nm which is red-shifted compared to that for **3** (λ_{em} = 516 nm), the emission spectrum of **2** shows a blue-shifted band at 503 nm (Figure 2). The emission lifetimes of 3.0 and 0.6 μs for **1** and **2**, respectively, confirm the phosphorescence origin of the emission. The phosphorescence band of **4** appears at a high energy region (493 nm), similar to that observed for other fluoro-substituted $(C^{\wedge}N)_2$Ir(acac) complexes.[31,33,34] Despite the electron-deficient nature of carborane, the large difference of about 40 nm (1450 cm^{-1}) between the emission wavelengths of **1** and **4** is quite unusual. The blue shift of 13 nm (501 cm^{-1}) observed for **2** in comparison with the emission wavelength of **3** is also pronounced. These results indicate that a change in the position of the carborane substituent on the phenyl ring can lead to phosphorescence color tuning. The phosphorescence spectra of **1** and **2**, which lack vibronic structure, closely resemble the spectra of **3** and **4**, suggesting that the lowest energy excited state of **1** and **2** is mainly ^{3}MLCT in character. The small Stokes shifts between λ_{max} for the ^{3}MLCT absorption and emission bands for **1** (57 nm, ~2260 cm^{-1}) and **2** (52 nm, ~2290 cm^{-1}) further support this assignment, as similarly found in *ppy*-ligand containing Ir(III) complexes.[8] Inspection of the phosphorescence quantum efficiencies indicates that the 4-substituted **1** is much less emissive than the 5-substituted **2** (Table 1). The reason for this is not understood, but might be partly related to the small HOMO–LUMO band gap of **1**, which may facilitate the nonradiative decay processes according to the energy-gap law.[35] In addition, we observe from TD-DFT calculation that the triplet state of **1** is significantly stabilized by a major contribution from the carborane (see below). This might retard the radiative decay process, as consistent with the relatively long emission lifetime of **1**.

Electrochemistry. The electrochemical properties of **1** and **2** were examined by cyclic voltammetry (Table 1 and Figure 3). Compounds **1** and **2** undergo reversible oxidation at 0.51 and 0.55 V, respectively. Interestingly, these oxidation potentials are anodically shifted in comparison with those of **3** (0.41 V)[31] and **4** (0.46 V), indicating that the HOMO of **1** and **2** is lower in energy than **3** and **4**, probably because of the effective stabilization of the HOMO by the inductive effect of carborane (see also DFT results). On the other hand, **1** and **2** display reduction processes that are chemically reversible but electrochemically quasi-reversible. Since it is known that aryl substituted-*o*-carboranes typically undergo a reduction in a range similar to that observed for **1** and **2**,[13,36] this reduction feature could be a consequence of the involvement of the carborane in the pyridyl reduction, which, in turn, implies that the carborane may affect the LUMO level. Although the reduction process in **4** was not observed in this study, one may assume that the reduction would occur in the range of −2.4 ~ −2.6 V because the $(4,6\text{-}dfppy)_2$Ir(acac) complex is reported to undergo reduction at −2.44 V.[31] Thus, comparison of the reduction potentials indicates that reduction of **1** is the most facile among the complexes, reflecting significant LUMO stabilization in **1**. Considering that the reduction process mainly involves the π^* orbital of the pyridyl ring fragment in $(C^{\wedge}N)_2$Ir(acac) complexes, such a LUMO stabilization by carborane substitution on the phenyl ring is remarkable. Although less than **1**, complex **2** similarly shows a low reduction potential, indicating that the carborane at the 5-

Table 3. Device Performance of PhOLEDs.[a]

device	emitter	CIE (x, y)[b]	$V_{turn\text{-}on}$ (V)[c]	L_{max} (cd/m^2)[d]	EQE$_{max}$ (%)[e]	PE$_{max}$ (lm/W)[f]
D1	**1**	(0.392, 0.585)	4.6	13300	6.6	10.7
D2	*fac*-Ir(ppy)$_3$	(0.330, 0.612)	3.4	40100	10.9	25.0

[a]Device structure: ITO/NPB (40 nm)/CBP:emitter (8 wt %) (30 nm)/BCP (10 nm)/Alq$_3$ (40 nm)/LiF (1 nm)/Al (100 nm). [b]Measured at 10 mA/cm^2-current density. [c]Applied voltage at the luminance of 1 cd/m^2. [d]Maximum luminance. [e]Maximum external quantum efficiency. [f]Maximum power efficiency.

dx.doi.org/10.1021/ic3015699 | *Inorg. Chem.* 2013, 52, 160–168

position of phenyl ring also contributes to LUMO stabilization. This reduction behavior in **1** and **2** may be related to the strong inductive electron-withdrawing effect of carborane, as well as to the participation of carborane in the LUMO delocalization.

Theoretical Calculations. To elucidate the photophysical and electrochemical properties of **1** and **2** discussed above, TD-DFT calculations on both the ground state (S_0) and lowest triplet excited state (T_1) optimized structures of **1** were performed at the B3LYP/LANL2DZ level (Figure 4 and Table 2). We find that the lowest energy absorption is mainly characterized by a HOMO−LUMO transition. While the HOMO resides on both the π orbital on the phenyl ring of the ligand (32.8%) and Ir(d_π) (53.5%), the LUMO is located on the *C^N* ligand and has the following contributions: pyridyl ring (52.8%), phenyl ring (30.2%), and carboranyl carbon atoms (12.6%). This suggests that the lowest energy absorption is mainly MLCT in character with substantial contribution from ligand-centered $\pi-\pi^*$ transition, and the LUMO could be significantly stabilized by the contribution from the carboranyl carbon atoms. The calculated LUMO level for **1** (−2.04 eV) is much lower than that of the reported value for **3** (−1.57 eV) at the same level of theory.[9] This feature is essentially the same as that found in the triarylboranes bearing *o*-carborane.[13,14] In contrast, the HOMO in **1** has little contribution from the 4-position of the phenyl ring, indicating that there might be no additional stabilization by delocalization through the carborane. Nevertheless, the calculated HOMO level of −5.51 eV is still lower than that of **3** (−5.08 eV), pointing to the presence of a strong inductive electron-withdrawing effect of carborane. Indeed, these results are consistent with the electrochemical data of **1**. Although the extent of the inductive effect exerted by the carborane on the HOMO and LUMO could not be exactly estimated, the resulting HOMO−LUMO band gap of **1** is narrowed by 0.04 eV because of more LUMO stabilization than that of **3**. This result may correlate with the observed red shift (10 nm, 595 cm^{-1}) of the lowest singlet absorption for **1**. In the case of the 4-fluoro-substituted **4**, while the strong inductive effect of the fluorine atom substantially lowers the HOMO level, the stabilization of the LUMO level does not appear pronounced, owing to a weak π donation from the p-orbital of fluorine to the LUMO through the 4-position. The reported calculation data for **4** is also consistent with this hypothesis.[9] Consequently, the increased band gap may lead to blue shift of the absorption band, as shown in Figure 2.

The blue shift observed in the absorption band of 5-carborane substituted **2** could be similarly explained by the orbital analyses described for **1**. While the HOMO electron density at the 5-position of the phenyl ring would be effectively stabilized by the inductive effect of carborane, the absence of a LUMO contribution from carborane at the 5-position could hardly lead to the lowering of the LUMO level by as much as in **1**. Accordingly, the band gap is increased to afford a blue shift of the absorption band. In fact, this feature is in good agreement with the electrochemical data of **1** and **2**, that is, **2** has slightly higher oxidation and reduction potentials than does **1**. This 5-substitution effect of carborane is in contrast to the 5-fluorine substituted Ir(III)[34] and Pt(II)[6] complexes in which a marginal blue shift or even a red shift upon 5-fluoro-substitution is observed owing to the offset of the inductive effect of the fluorine atom by π donation into the HOMO.

Next, the TD-DFT calculations at the T_1 optimized geometry for **1** show that the lowest energy triplet state is also dominated by a HOMO−LUMO transition. As shown in Figure 4 (right), the HOMO is localized on both the phenyl ring of the ligand and the Ir atom, with similar contributions as observed in the ground state structure. However, it can be seen that the LUMO bears a large contribution from the carborane (54.3%) with full delocalization over the ligand. As a result, the LUMO energy level is significantly stabilized (−2.76 eV vs −2.04 eV at the S_0 state), while the HOMO level is changed little (−5.43 eV vs −5.51 eV at the S_0) in accordance with the red-shifted phosphorescence band of **1**. Furthermore, this feature indicates that the lowest triplet state (T_1) is governed by the carborane and thus has $[d_\pi(Ir)\rightarrow\pi^*(C^\wedge N)]$ ^{3}MLCT character with some contribution from ^{3}LC. The calculated $T_1 \rightarrow S_0$ transition is also in good agreement with the observed phosphorescence band (Table 2).

Electroluminescent Properties. To explore the possibility of using **1** and **2** as an emitting material in phosphorescent OLEDs (PhOLEDs), devices based on emissive layers containing a 9,9′-(1,1′-biphenyl)-4,4′-diylbis-9*H*-carbazole (CBP) (E_T = 2.56 eV)[37,38] host doped with **1** (E_T = 2.37 eV from 0−0 phosphorescence at 77 K) or **2** (E_T = 2.51 eV) were fabricated by vacuum deposition with the following configuration: ITO/NPB (40 nm)/CBP:emitter (8 wt %) (30 nm)/BCP (10 nm)/Alq_3 (40 nm)/LiF (1 nm)/Al (100 nm), where NPB is *N*,*N*′-bis(naphthalene-1-yl)-*N*,*N*′-bis(phenyl)-benzidine,[39] CBP is 4,4′-bis(9-carbazolyl)-biphenyl, BCP is bathocuproine,[40] and Alq_3 is tris(8-hydroxyquinolinolato)-aluminum. Unfortunately, it was found that **2** undergoes thermal decomposition during the course of vacuum sublimation, thus only a device incorporating **1** (**D1**) was tested. A reference device **D2** with the well-known *fac*-Ir(ppy)$_3$ emitter was also fabricated in the identical device structure.[38]

As shown in Figure 5, **D1** emits green light (λ_{em} = 536 nm), which is very similar to the PL spectrum of **1**, indicating that light emission originates only from phosphorescent dopant **1**. The electroluminescence (EL) spectra obtained at various current densities ranging from 10 to 100 mA/cm^2 do not exhibit much change except for a gradual increase in the emission intensity, indicating stable light emission. According to the EL characteristics (Figure 6 and Table 3), the turn-on voltage of **D1** (4.6 V) was somewhat higher than that of device **D2** (3.4 V). With the increasing applied voltage, **D1** showed a high level of current density and luminance with a maximum brightness (L_{max}) of 13,300 cd/m^2 at 12.0 V. The lifetime tests for **D1** and **D2** under the constant current yielding the initial luminance of 200 cd/m^2 indicate that the devices based on **1** exhibit high level of stability comparable to that of *fac*-Ir(ppy)$_3$-based devices (Supporting Information, Figure S5). Although **D1** displayed overall good performance in terms of external quantum efficiency (η_{EQE}, 6.6%) and power efficiency (η_{PE}, 10.7 lm/W), these were still inferior to the performance of the **D2** device (Table 3 and Supporting Information, Figure S6 for EL characteristics for **D2**). As seen from the low PL quantum efficiency of **1**, the stabilization of triplet excitons or charge carrier (electron) trapping by the carborane is likely to cause an imbalance between electrons and holes, resulting in the observed lower device performance.

CONCLUSION

The introduction of an *o*-carborane to the 4- and 5-position of the phenyl ring of a *ppy* ligand in heteroleptic $(C^\wedge N)_2$Ir(acac) complexes gave rise to red and blue shifts of the phosphorescence band, respectively, compared to that of $(ppy)_2$Ir(acac). We find from electrochemical and theoretical

dx.doi.org/10.1021/ic3015699 | *Inorg. Chem.* 2013, 52, 160−168

studies that a carborane substitution on the 4-position of the phenyl ring lowers the ^{3}MLCT energy by LUMO stabilization via the contribution of the carborane to LUMO delocalization, while substitution on the 5-position raises the ^{3}MLCT energy by the stabilization of the HOMO level because of the strong inductive electron-withdrawing effect of carborane. An EL device incorporating the 4-carborane substituted Ir(III) complex displayed overall good performance with green phosphorescence, suggesting that this type of complex could potentially be useful as phosphorescent emitter in PhOLEDs.

■ ASSOCIATED CONTENT

Supporting Information

Crystallographic data for **1** in cif format, additional UV−vis, PL, and EL data, and computational details. This material is available free of charge via the Internet at http://pubs.acs.org.

■ AUTHOR INFORMATION

Corresponding Author

*E-mail: YoonSupLee@kaist.ac.kr (Y.S.L.), lmh74@ulsan.ac.kr (M.H.L.).

Notes

The authors declare no competing financial interest.

■ ACKNOWLEDGMENTS

This work was supported by the Basic Science Research Program (No. 2012039773 for M.H.L. and No. 2007-0056341 for Y.S.L.) and Priority Research Centers Program (No. 2009-0093818 for M.H.L.) through the National Research Foundation of Korea (NRF) funded by the Ministry of Education, Science and Technology. Computational resources for this work were provided by KISTI (KSC-2011-C2-18). We thank Dongwoo FineChem Co. for assisting with the EL measurements.

■ REFERENCES

(1) Baranoff, E.; Jung, I.; Scopelliti, R.; Solari, E.; Grätzel, M.; Nazeeruddin, M. K. *Dalton Trans.* **2011**, *40*, 6860−6867.

(2) Chi, Y.; Chou, P.-T. *Chem. Soc. Rev.* **2010**, *39*, 638−655. You, Y.; Park, S. Y. *Dalton Trans.* **2009**, 1267−1282. Flamigni, L.; Barbieri, A.; Sabatini, C.; Ventura, B.; Barigelletti, F. *Top. Curr. Chem.* **2007**, *281*, 143−203. Chou, P.-T.; Chi, Y. *Chem.—Eur. J.* **2007**, *13*, 380−395. Ma, B.; Djurovich, P. I.; Thompson, M. E. *Coord. Chem. Rev.* **2005**, *249*, 1501−1510. Holder, E.; Langeveld, B. M. W.; Schubert, U. S. *Adv. Mater.* **2005**, *17*, 1109−1121. Yersin, H. *Top. Curr. Chem.* **2004**, *241*, 1−26. Adachi, C.; Baldo, M. A.; Forrest, S. R.; Thompson, M. E. *Appl. Phys. Lett.* **2000**, *77*, 904−906. Baldo, M. A.; Thompson, M. E.; Forrest, S. R. *Nature* **2000**, *403*, 750−753.

(3) Yang, X.; Zhao, Y.; Zhang, X.; Li, R.; Dang, J.; Li, Y.; Zhou, G.; Wu, Z.; Ma, D.; Wong, W.-Y.; Zhao, X.; Ren, A.; Wang, L.; Hou, X. *J. Mater. Chem.* **2012**, *22*, 7136−7148. Zhu, M.; Li, Y.; Hu, S.; Li, C. g.; Yang, C.; Wu, H.; Qin, J.; Cao, Y. *Chem. Commun.* **2012**, *48*, 2695−2697. Kuwabara, J.; Namekawa, T.; Haga, M.-a.; Kanbara, T. *Dalton Trans.* **2012**, *41*, 44−46. Lu, K.-Y.; Chou, H.-H.; Hsieh, C.-H.; Yang, Y.-H. O.; Tsai, H.-R.; Tsai, H.-Y.; Hsu, L.-C.; Chen, C.-Y.; Chen, I. C.; Cheng, C.-H. *Adv. Mater.* **2011**, *23*, 4933−4937. Chen, S.; Tan, G.; Wong, W.-Y.; Kwok, H.-S. *Adv. Funct. Mater.* **2011**, *21*, 3785−3793. Hudson, Z. M.; Helander, M. G.; Lu, Z.-H.; Wang, S. *Chem. Commun.* **2011**, *47*, 755−757. Bolink, H. J.; De Angelis, F.; Baranoff, E.; Klein, C.; Fantacci, S.; Coronado, E.; Sessolo, M.; Kalyanasundaram, K.; Grätzel, M.; Nazeeruddin, M. K. *Chem. Commun.* **2009**, 4672−4674. Sajoto, T.; Djurovich, P. I.; Tamayo, A. B.; Oxgaard, J.; Goddard, W. A.; Thompson, M. E. *J. Am. Chem. Soc.* **2009**, *131*, 9813−9822. Zhou, G.; Ho, C.-L.; Wong, W.-Y.; Wang, Q.; Ma, D.; Wang, L.; Lin, Z.; Marder, T. B.; Beeby, A. *Adv. Funct. Mater.* **2008**, *18*, 499−511. Park, Y.-S.; Kang, J.-W.; Kang, D. M.; Park, J.-W.; Kim, Y.-H.; Kwon, S.-K.; Kim, J.-J. *Adv. Mater.* **2008**, *20*, 1957−1961. Yang, X.; Wang, Z.; Madakuni, S.; Li, J.; Jabbour, G. E. *Adv. Mater.* **2008**, *20*, 2405−2409. Williams, E. L.; Haavisto, K.; Li, J.; Jabbour, G. E. *Adv. Mater.* **2007**, *19*, 197−202. Zhao, Q.; Liu, S.; Shi, M.; Wang, C.; Yu, M.; Li, L.; Li, F.; Yi, T.; Huang, C. *Inorg. Chem.* **2006**, *45*, 6152−6160. Yu, X.-M.; Kwok, H.-S.; Wong, W.-Y.; Zhou, G.-J. *Chem. Mater.* **2006**, *18*, 5097−5103. Sajoto, T.; Djurovich, P. I.; Tamayo, A.; Yousufuddin, M.; Bau, R.; Thompson, M. E.; Holmes, R. J.; Forrest, S. R. *Inorg. Chem.* **2005**, *44*, 7992−8003. Li, J.; Djurovich, P. I.; Alleyne, B. D.; Yousufuddin, M.; Ho, N. N.; Thomas, J. C.; Peters, J. C.; Bau, R.; Thompson, M. E. *Inorg. Chem.* **2005**, *44*, 1713−1727. D'Andrade, B. W.; Forrest, S. R. *Adv. Mater.* **2004**, *16*, 1585−1595. D'Andrade, B. W.; Holmes, R. J.; Forrest, S. R. *Adv. Mater.* **2004**, *16*, 624−628. Furuta, P. T.; Deng, L.; Garon, S.; Thompson, M. E.; Fréchet, J. M. J. *J. Am. Chem. Soc.* **2004**, *126*, 15388−15389.

(4) Kui, S. C. F.; Hung, F.-F.; Lai, S.-L.; Yuen, M.-Y.; Kwok, C.-C.; Low, K.-H.; Chui, S. S.-Y.; Che, C.-M. *Chem.—Eur. J.* **2012**, *18*, 96−109. Lin, C.-H.; Chi, Y.; Chung, M.-W.; Chen, Y.-J.; Wang, K.-W.; Lee, G.-H.; Chou, P.-T.; Hung, W.-Y.; Chiu, H.-C. *Dalton Trans.* **2011**, *40*, 1132−1143. Chiu, Y.-C.; Hung, J.-Y.; Chi, Y.; Chen, C.-C.; Chang, C.-H.; Wu, C.-C.; Cheng, Y.-M.; Yu, Y.-C.; Lee, G.-H.; Chou, P.-T. *Adv. Mater.* **2009**, *21*, 2221−2225. Chiu, Y.-C.; Lin, C.-H.; Hung, J.-Y.; Chi, Y.; Cheng, Y.-M.; Wang, K.-W.; Chung, M.-W.; Lee, G.-H.; Chou, P.-T. *Inorg. Chem.* **2009**, *48*, 8164−8172. Xu, M.; Wang, G.; Zhou, R.; An, Z.; Zhou, Q.; Li, W. *Inorg. Chim. Acta* **2007**, *360*, 3149−3154. You, Y.; An, C.-G.; Kim, J.-J.; Park, S. Y. *J. Org. Chem.* **2007**, *72*, 6241−6246. Tamayo, A. B.; Alleyne, B. D.; Djurovich, P. I.; Lamansky, S.; Tsyba, I.; Ho, N. N.; Bau, R.; Thompson, M. E. *J. Am. Chem. Soc.* **2003**, *125*, 7377−7387. Tsuboyama, A.; Iwawaki, H.; Furugori, M.; Mukaide, T.; Kamatani, J.; Igawa, S.; Moriyama, T.; Miura, S.; Takiguchi, T.; Okada, S.; Hoshino, M.; Ueno, K. *J. Am. Chem. Soc.* **2003**, *125*, 12971−12979. Grushin, V. V.; Herron, N.; LeCloux, D. D.; Marshall, W. J.; Petrov, V. A.; Wang, Y. *Chem. Commun.* **2001**, 1494−1495.

(5) Edkins, R. M.; Wriglesworth, A.; Fucke, K.; Bettington, S. L.; Beeby, A. *Dalton Trans.* **2011**, *40*, 9672−9678.

(6) Brooks, J.; Babayan, Y.; Lamansky, S.; Djurovich, P. I.; Tsyba, I.; Bau, R.; Thompson, M. E. *Inorg. Chem.* **2002**, *41*, 3055−3066.

(7) Lamansky, S.; Djurovich, P.; Murphy, D.; Abdel-Razzaq, F.; Kwong, R.; Tsyba, I.; Bortz, M.; Mui, B.; Bau, R.; Thompson, M. E. *Inorg. Chem.* **2001**, *40*, 1704−1711.

(8) Lamansky, S.; Djurovich, P.; Murphy, D.; Abdel-Razzaq, F.; Lee, H. E.; Adachi, C.; Burrows, P. E.; Forrest, S. R.; Thompson, M. E. *J. Am. Chem. Soc.* **2001**, *123*, 4304−4312.

(9) Liu, T.; Xia, B.-H.; Zhou, X.; Zheng, Q.-C.; Pan, Q.-J.; Zhang, H.-X. *Theoret. Chim. Acta.* **2008**, *121*, 155−164.

(10) Takizawa, S.-Y.; Nishida, J.-I.; Tsuzuki, T.; Tokito, S.; Yamashita, Y. *Inorg. Chem.* **2007**, *46*, 4308−4319. Djurovich, P. I.; Murphy, D.; Thompson, M. E.; Hernandez, B.; Gao, R.; Hunt, P. L.; Selke, M. *Dalton Trans.* **2007**, 3763−3770. Zhao, Q.; Cao, T.; Li, F.; Li, X.; Jing, H.; Yi, T.; Huang, C. *Organometallics* **2007**, *26*, 2077−2081. Park, N. G.; Choi, G. C.; Lee, Y. H.; Kim, Y. S. *Curr. Appl. Phys.* **2006**, *6*, 620−626. Jung, S. O.; Kang, Y.; Kim, H.-S.; Kim, Y.-H.; Yang, K.; Kwon, S.-K. *Bull. Korean Chem. Soc.* **2003**, *24*, 1521−1524. Hay, P. J. *J. Phys. Chem. A* **2002**, *106*, 1634−1641.

(11) Chen, Z.; King, R. B. *Chem. Rev.* **2005**, *105*, 3613−3642. King, R. B. *Chem. Rev.* **2001**, *101*, 1119−1152. Hawthorne, M. F. *Advances in Boron Chemistry: Special Publication No. 201*; Royal Society of Chemistry: London, U.K., 1997; Vol. *82*, p 261; Williams, R. E. *Chem. Rev.* **1992**, *92*, 177−207.

(12) Hosmane, N. S. *Boron Science: New Technologies and Applications*; CRC Press: New York, 2012; Dash, B. P.; Satapathy, R.; Gaillard, E. R.; Norton, K. M.; Maguire, J. A.; Chug, N.; Hosmane, N. S. *Inorg. Chem.* **2011**, *50*, 5485−5493. Kokado, K.; Chujo, Y. *Dalton Trans.* **2011**, *40*, 1919−1923. Park, M. H.; Lee, K. M.; Kim, T.; Do, Y.; Lee, M. H. *Chem. Asian J.* **2011**, *6*, 1362−1366. Kokado, K.; Chujo, Y. *J. Org. Chem.* **2011**, *76*, 316−319. Dash, B. P.; Satapathy, R.; Gaillard, E. R.; Maguire, J. A.; Hosmane, N. S. *J. Am. Chem. Soc.* **2010**, *132*, 6578−6587. Kokado, K.; Tokoro, Y.; Chujo, Y. *Macromolecules* **2009**,

42, 9238−9242. Peterson, J. J.; Werre, M.; Simon, Y. C.; Coughlin, E. B.; Carter, K. R. *Macromolecules* **2009**, *42*, 8594−8598. Kokado, K.; Tokoro, Y.; Chujo, Y. *Macromolecules* **2009**, *42*, 2925−2930. Peterson, J. J.; Simon, Y. C.; Coughlin, E. B.; Carter, K. R. *Chem. Commun.* **2009**, 4950−4952. Kokado, K.; Chujo, Y. *Macromolecules* **2009**, *42*, 1418−1420.

(13) Lee, K. M.; Huh, J. O.; Kim, T.; Do, Y.; Lee, M. H. *Dalton Trans.* **2011**, *40*, 11758−11764.

(14) Huh, J. O.; Kim, H.; Lee, K. M.; Lee, Y. S.; Do, Y.; Lee, M. H. *Chem. Commun.* **2010**, *46*, 1138−1140.

(15) Malamas, M. S.; Barnes, K.; Johnson, M.; Hui, Y.; Zhou, P.; Turner, J.; Hu, Y.; Wagner, E.; Fan, K.; Chopra, R.; Olland, A.; Bard, J.; Pangalos, M.; Reinhart, P.; Robichaud, A. J. *Bioorg. Med. Chem.* **2010**, *18*, 630−639.

(16) Schwab, P. F. H.; Fleischer, F.; Michl, J. *J. Org. Chem.* **2002**, *67*, 443−449. Zhang, B.; Breslow, R. *J. Am. Chem. Soc.* **1997**, *119*, 1676−1681.

(17) Shavaleev, N. M.; Monti, F.; Costa, R. D.; Scopelliti, R.; Bolink, H. J.; Ortí, E.; Accorsi, G.; Armaroli, N.; Baranoff, E.; Grätzel, M.; Nazeeruddin, M. K. *Inorg. Chem.* **2012**, *51*, 2263−2271. Cline, E. D.; Adamson, S. E.; Bernhard, S. *Inorg. Chem.* **2008**, *47*, 10378−10388.

(18) Sheldrick, G. M. *SHELXL-93: Program for the refinement of crystal structures*; University of Göttingen: Göttingen, Germany, 1993.

(19) Brouwer, A. M. *Pure Appl. Chem.* **2011**, *83*, 2213−2228. Melhuish, W. H. *J. Phys. Chem.* **1961**, *65*, 229−235.

(20) Ahire, J. H.; Wang, Q.; Coxon, P. R.; Malhotra, G.; Brydson, R.; Chen, R.; Chao, Y. *ACS Appl. Mater. Interfaces* **2012**, *4*, 3285−3292.

(21) Runge, E.; Gross, E. K. U. *Phys. Rev. Lett.* **1984**, *52*, 997−1000.

(22) Stephens, P. J.; Devlin, F. J.; Chabalowski, C. F.; Frisch, M. J. *J. Phys. Chem.* **1994**, *98*, 11623−11627. Lee, C.; Yang, W.; Parr, R. G. *Phys. Rev. B* **1988**, *37*, 785−789.

(23) Francl, M. M.; Pietro, W. J.; Hehre, W. J.; Binkley, J. S.; Gordon, M. S.; DeFrees, D. J.; Pople, J. A. *J. Chem. Phys.* **1982**, *77*, 3654−3665. Hariharan, P. C.; Pople, J. A. *Theoret. Chim. Acta.* **1973**, *28*, 213−222. Hehre, W. J.; Ditchfield, R.; Pople, J. A. *J. Chem. Phys.* **1972**, *56*, 2257−2261.

(24) Hay, P. J.; Wadt, W. R. *J. Chem. Phys.* **1985**, *82*, 270−283.

(25) Frisch, M. J. T., G. W.; Schlegel, H. B.; Scuseria, G. E.; Robb, M. A.; Cheeseman, J. R.; Montgomery, J. A. Jr.; Vreven, T.; Kudin, K. N.; Burant, J. C.; Millam, J. M.; Iyengar, S. S.; Tomasi, J.; Barone, V.; Mennucci, B.; Cossi, M.; Scalmani, G.; Rega, N.; Petersson, G. A.; Nakatsuji, H.; Hada, M.; Ehara, M.; Toyota, K.; Fukuda, R.; Hasegawa, J.; Ishida, M.; Nakajima, T.; Honda, Y.; Kitao, O.; Nakai, H.; Klene, M.; Li, X.; Knox, J. E.; Hratchian, H. P.; Cross, J. B.; Bakken, V.; Adamo, C.; Jaramillo, J.; Gomperts, R.; Stratmann, R. E.; Yazyev, O.; Austin, A. J.; Cammi, R.; Pomelli, C.; Ochterski, J. W.; Ayala, P. Y.; Morokuma, K.; Voth, G. A.; Salvador, P.; Dannenberg, J. J.; Zakrzewski, V. G.; Dapprich, S.; Daniels, A. D.; Strain, M. C.; Farkas, O.; Malick, D. K.; Rabuck, A. D.; Raghavachari, K.; Foresman, J. B.; Ortiz, J. V.; Cui, Q.; Baboul, A. G.; Clifford, S.; Cioslowski, J.; Stefanov, B. B.; Liu, G.; Liashenko, A.; Piskorz, P.; Komaromi, I.; Martin, R. L.; Fox, D. J.; Keith, T.; Al-Laham, M. A.; Peng, C. Y.; Nanayakkara, A.; Challacombe, M.; Gill, P. M. W.; Johnson, B.; Chen, W.; Wong, M. W.; Gonzalez, C.; Pople, J. A. *Gaussian 09*, Revision A.02; Gaussian, Inc.: Wallingford, CT, 2009.

(26) Jiang, W.; Knobler, C. B.; Hawthorne, M. F. *Inorg. Chem.* **1996**, *35*, 3056−3058. Hawthorne, M. F.; Berry, T. E.; Wegner, P. A. *J. Am. Chem. Soc.* **1965**, *87*, 4746−4750. Heying, T. L.; Ager, J. W.; Clark, S. L.; Mangold, D. J.; Goldstein, H. L.; Hillman, M.; Polak, R. J.; Szymanski, J. W. *Inorg. Chem.* **1963**, *2*, 1089−1092.

(27) Songkram, C.; Takaishi, K.; Yamaguchi, K.; Kagechika, H.; Endo, Y. *Tetrahedron Lett.* **2001**, *42*, 6365−6368. Lamrani, M.; Hamasaki, R.; Mitsuishi, M.; Miyashita, T.; Yamamoto, Y. *Chem. Commun.* **2000**, 1595−1596. Kabalka, G. W.; Reddy, N. K.; Narayana, C. *Tetrahedron Lett.* **1992**, *33*, 7687−7688.

(28) Li, L.; Brennessel, W. W.; Jones, W. D. *Organometallics* **2009**, *28*, 3492−3500.

(29) Evans, N. R.; Devi, L. S.; Mak, C. S. K.; Watkins, S. E.; Pascu, S. I.; Köhler, A.; Friend, R. H.; Williams, C. K.; Holmes, A. B. *J. Am. Chem. Soc.* **2006**, *128*, 6647−6656.

(30) Vadavi, R. S.; Kim, H.; Lee, K. M.; Kim, T.; Lee, J.; Lee, Y. S.; Lee, M. H. *Organometallics* **2012**, *31*, 31−34. Rai, V. K.; Nishiura, M.; Takimoto, M.; Hou, Z. *Chem. Commun.* **2011**, *47*, 5726−5728. Shin, C. H.; Huh, J. O.; Lee, M. H.; Do, Y. *Dalton Trans.* **2009**, 6476−6479. Zhao, Q.; Li, L.; Li, F.; Yu, M.; Liu, Z.; Yi, T.; Huang, C. *Chem. Commun.* **2008**, 685−687. Sie, W.-S.; Jian, J.-Y.; Su, T.-C.; Lee, G.-H.; Lee, H. M.; Shiu, K.-B. *J. Organomet. Chem.* **2008**, *693*, 1510−1517. Orselli, E.; Kottas, G. S.; Konradsson, A. E.; Coppo, P.; Fröhlich, R.; De Cola, L.; van Dijken, A.; Büchel, M.; Börner, H. *Inorg. Chem.* **2007**, *46*, 11082−11093.

(31) Baranoff, E.; Curchod, B. F. E.; Frey, J.; Scopelliti, R.; Kessler, F.; Tavernelli, I.; Rothlisberger, U.; Grätzel, M.; Nazeeruddin, M. K. *Inorg. Chem.* **2012**, *51*, 215−224.

(32) Schmid, B.; Garces, F. O.; Watts, R. J. *Inorg. Chem.* **1994**, *33*, 9−14. Colombo, M. G.; Hauser, A.; Güdel, H. U. *Top. Curr. Chem.* **1994**, *171*, 143−171. Colombo, M. G.; Hauser, A.; Guedel, H. U. *Inorg. Chem.* **1993**, *32*, 3088−3092.

(33) Rausch, A. F.; Thompson, M. E.; Yersin, H. *J. Phys. Chem. A* **2009**, *113*, 5927−5932. Adachi, C.; Kwong, R. C.; Djurovich, P.; Adamovich, V.; Baldo, M. A.; Thompson, M. E.; Forrest, S. R. *Appl. Phys. Lett.* **2001**, *79*, 2082−2084.

(34) Ragni, R.; Plummer, E. A.; Brunner, K.; Hofstraat, J. W.; Babudri, F.; Farinola, G. M.; Naso, F.; De Cola, L. *J. Mater. Chem.* **2006**, *16*, 1161−1170.

(35) Lakowicz, J. R. *Principles of Fluorescence Spectroscopy*, 3rd ed.; Springer: New York, 2006; pp 687−688.

(36) Tricas, H.; Colon, M.; Ellis, D.; Macgregor, S. A.; McKay, D.; Rosair, G. M.; Welch, A. J.; Glukhov, I. V.; Rossi, F.; Laschi, F.; Zanello, P. *Dalton Trans.* **2011**, *40*, 4200−4211. Fox, M. A.; Nervi, C.; Crivello, A.; Batsanov, A. S.; Howard, J. A. K.; Wade, K.; Low, P. J. *J. Solid State Electron.* **2009**, *13*, 1483−1495. Fox, M. A.; Nervi, C.; Crivello, A.; Low, P. J. *Chem. Commun.* **2007**, 2372−2374.

(37) Brunner, K.; van Dijken, A.; Börner, H.; Bastiaansen, J. J. A. M.; Kiggen, N. M. M.; Langeveld, B. M. W. *J. Am. Chem. Soc.* **2004**, *126*, 6035−6042.

(38) Baldo, M. A.; Lamansky, S.; Burrows, P. E.; Thompson, M. E.; Forrest, S. R. *Appl. Phys. Lett.* **1999**, *75*, 4−6.

(39) Van Slyke, S. A.; Chen, C. H.; Tang, C. W. *Appl. Phys. Lett.* **1996**, *69*, 2160−2162.

(40) O'Brien, D. F.; Baldo, M. A.; Thompson, M. E.; Forrest, S. R. *Appl. Phys. Lett.* **1999**, *74*, 442−444.